15TH IEA HEAT PUMP CONFERENCE
MAY 26–29, 2026 | HOFBURG
VIENNA 2026
DECARBONISATION THROUGH INNOVATION

Control strategies for constant supply temperature of a high-temperature Brayton heat pump

Johannes Drews (né Oehler)[1*], A. Phong Tran[1], Fatma Cansu Yücel[1], Panagiotis Stathopoulos[1]

[1]German Aerospace Center (DLR), Institute of Low-Carbon Industrial Processes, Cottbus, Germany

---

Abstract

High-temperature heat pumps are the most efficient and potentially emission free option to supply process heat at temperature levels up to 300 °C. Many industrial processes require high-temperature heat but at the same time reliable, and controllable process heat parameters even under varying load conditions such as mass flow or inlet temperature variations. The Brayton heat pump facility "CoBra" is a demonstrator for a closed-loop high-temperature heat pump using dry air as working fluid. It can supply sensible heat to process air streams at temperatures above 200 °C. In order to be a viable heat supply option for industrial processes, a suitable control method to ensure precise temperature control must be identified and evaluated. In this work, an experimental campaign with two different control strategies for process temperature control is conducted and the results subsequently compared. A variation of the fluid inventory and compressor speed are used to control the process temperature. Both control methods are capable of maintaining a constant process temperature of e.g. 200 °C $\pm$ 2 °C in case of occurring perturbations. Variations of the set point temperature are also achievable with both controllers. Overshoots can be eliminated by choosing appropriate controller parameters. The results show that compressor speed control is faster in achieving a new set point process temperature compared to the fluid inventory change. A constant process temperature can be maintained despite a reduction in fluid inventory with an appropriate increase in compressor speed. This indicates that the two controllers can compensate for each other's effect on the process temperature. Controller performance could be further improved by a rigorous and systematic parameter tuning.

Keywords: High-temperature heat pump, process heat, closed-loop Brayton cycle, controls

---

1 Introduction

In order to significantly decrease global CO_2 emissions, urgent action must be taken. Currently, heating and cooling account for more than 40% of global energy-related carbon dioxide emissions and hence, is a major contributor to global warming [1]. The industrial sector, however, makes up to 22% of the total emission [2] making the sector a critical target for decarbonization efforts. A substantial portion of this energy demand arises from process heat, much of which is currently supplied by fossil fuels. Electrification of heat supply, particularly through the deployment of high-temperature heat pumps (HTHPs), offers a promising pathway to reduce both energy consumption and greenhouse gas emissions in industry (see [1]). Recent heat pump developments have increased the achievable supply temperatures and broadened their application range. The IEA HPT Annex 58 report [3] presents demonstration cases with supply temperatures between 115 °C to 280 °C. With Technology Readiness Levels (TRL) from 4 to 9, these systems show that high-temperature heat

*Corresponding author: johannes.drews@dlr.de

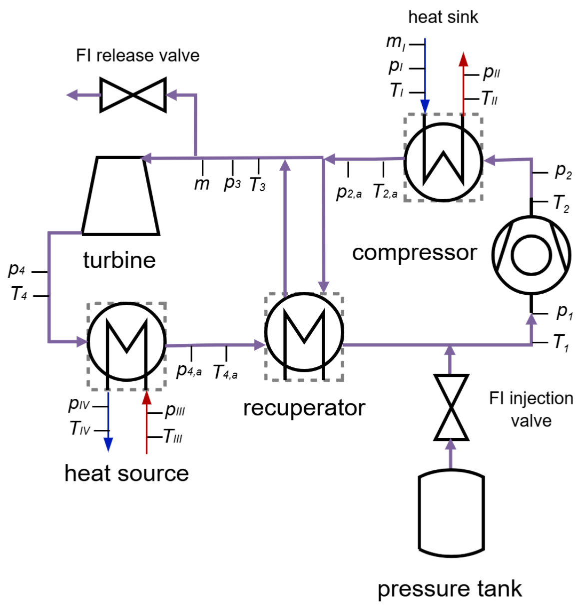

Figure 1: P&ID of the CoBra high temperature heat pump

pump technology is maturing and progressing towards commercial adoption. In order to make these systems suitable for the integration in existing industrial processes, HTHPs must deliver a stable and predictable heat output, even under fluctuating operating conditions. Hence, advanced control strategies capable of managing transient thermal behaviour are essential to ensure reliable system performance and process compatibility. Research on control strategies for closed-loop Brayton systems has primarily focused on two applications: supercritical CO_2 (sCO_2) power cycles and HTHPs. For sCO_2 Brayton systems, control methods are well-developed, with fluid inventory variation, compressor speed adjustment, and valve manipulation being the approaches investigated to meet power demands [4].

In contrast, Brayton heat pumps represent a newer technology with comparatively less developed control research. Similar to sCO_2 Brayton systems, fluid inventory and compressor speed variation emerge as the primary control mechanisms for these heat pumps. Pettinari et al. [5] examined both control strategies from a transient perspective, finding that rotational speed control achieves superior temperature tracking while inventory control is more advanced in preserving system performance across varying temperature glides. Oehler et al. [6] experimentally demonstrated that fluid inventory control widens the operational envelope of the heat pump's part-load operation while maintaining constant efficiency and compressor stability. Tran et al. [7] investigated the use of Reinforcement Learning controllers, trained on an experimentally validated dynamic model of a Brayton heat pump.

This work presents the first experimental validation of applying fluid inventory and compressor speed variation to control the thermal performance of a Brayton heat pump.

2 Experimental setup and methodology

All experiments in this study are carried out using the CoBra heat pump, which is described in detail by Yücel et al. [8]. [6] provides information on sensor types and accuracies. For completeness, a concise overview of the system and its thermodynamic cycle is provided in the following. The CoBra heat pump is an experimental demonstrator designed to validate the feasibility and performance of a closed-loop reverse Brayton cycle for high-temperature industrial heat supply. The system uses dry air as working fluid. The CoBra is built to provide cooling and heating simultaneously at temperature levels reaching up to 300°C and -40°C. A simplified piping and instrumentation diagram (P&ID) of the CoBra demonstrator is shown in Fig. 1. The primary Brayton loop comprises five main components: a two-stage centrifugal compressor, a two-stage axial turbine, and three shell-and-tube heat exchangers—a high-temperature heat exchanger (HTHX), a low-temperature heat exchanger (LTHX), and a recuperator. Two secondary loops simulate the heat sink and heat source, respectively. To prevent condensation or icing at sub-zero operating conditions, especially downstream of the turbine, dry air is used in the Brayton loop. Additional dry air can be injected into the heat pump through the FI (fluid inventory) injection valve from a pressure tank in order to compensate for leakage or to increase the fluid inventory.

The air in the Brayton loop is compressed using a two-stage centrifugal compression unit (Manufacturer:

ASA Kompressor GmbH), providing pressure ratios between 2.5 and 3.5. After compression the hot air flow enters the high-temperature heat exchanger (HTHX) where heat is being rejected to the heat sink. Downstream of the HTHX the air enters the recuperator. The cooled, pressurized air then expands through a two-stage axial turbine, producing mechanical work that is recovered via a generator and joint frequency converter to drive the compressor (see [8]). After expansion, the air passes through the low-temperature heat exchanger (LTHX), where it absorbs heat from the heat source and the recuperator before re-entering the compressor. The fluid inventory (FI) valve allows for releasing air to the environment from the Brayton loop, hence, enabling for the fluid inventory to be reduced during operation.

The control system of the CoBra heat pump uses two controllers to adjust its thermal performance:

Controller 1 – Compressor speed control The heat supply temperature is controlled by adjusting the rotational speed of the compressor n_C using a proportional-integral-differential (PID) controller. The PID controller manipulates the compressor speed setpoint based on the error $\Delta T_{\mathrm{II}} = T_{\mathrm{II,set}} - T_{\mathrm{II}}$ between the measured outlet temperature and its setpoint value. A change in compressor speed directly alters the mass flow rate of the working fluid and the pressure ratio, which consequently adjusts the compressor discharge temperature and therefore the achieved heat supply temperature.

Two variants of the controller are evaluated. An initial version employs a discrete-time, incremental logic. At fixed time steps Δt_1, if the temperature error exceeds a predefined tolerance $T_{II} \pm \Delta T_{\mathrm{tol}}$, the compressor speed is updated by an increment (Δn_{C}) calculated by Eq. (1) using a proportional-derivate action:

$$\Delta n_{\mathrm{C}} = K_P \cdot \Delta T_{\mathrm{II}} + K_d \cdot \frac{d}{dt}\Delta T_{\mathrm{II}} \tag{1}$$

Subsequent experiments utilize a standard continuous PID controller, that sets n_{C} according to Eq. (2):

$$n_C = K_P \cdot \left(\Delta T_{\mathrm{II}} + \frac{1}{T_i}\int_0^{\infty} \Delta T_{\mathrm{II}}\, dt + T_d \frac{d}{dt}\Delta T_{\mathrm{II}}\right) \tag{2}$$

Controller 2 – Fluid inventory control In addition, a fluid inventory control strategy is employed. This method allows for adjusting the total mass of working fluid within the closed loop. The control logic of the fluid inventory controller monitors the compressor inlet pressure p_1. Once the measured pressure falls outside of a range around the set point, one of the following actions is taken:

- Inventory increase: The fluid inventory is increased by introducing air from the buffer tank into the main cycle through an injection valve.
- Inventory decrease: The fluid inventory is decreased by discharging air from the loop via a release valve (see FI valve in Fig. 1).

In its default mode, this controller maintains a constant p_1 to compensate for leakages or pressure fluctuations caused by changes in compressor operation and thermal conditions.

Controller 2 can be extended to control the process temperature T_{II}. In this case, p_1 is modulated in fixed time steps Δt_2 according to Eq. (3) if the temperature leaves the tolerated temperature range $T_{\mathrm{II}} \pm \Delta T_{\mathrm{tol}}$:

$$\Delta p_1 = K_P \cdot \Delta T_{\mathrm{II}} + K_d \cdot \frac{d}{dt}\Delta T_{\mathrm{II}} \tag{3}$$

An increase of p_1 leads to an increased air inventory and hence an increased primary mass flow $\dot{m}$. This leads to a decrease of the HTHX mass flow ratio $\frac{\dot{m}_I}{\dot{m}}$ and consequently an increase of T_{2a}. The increase of T_{2a} leads to an increase of compressor inlet temperature T_1 via the recuperator and further an increase of compressor outlet temperature T_2 and process temperature T_{II}. This mechanism has the opposite effect for reduction of p_1 and explains how a change of fluid inventory affects the process temperature T_{II}.

Control setup Both controllers can be used to maintain a specific process temperature T_{II}. However, only one controller at a time is given the task of process temperature control.

In order to find the operating conditions with the highest coefficient of performance (COP) both controllers are activated simultaneously in Experiment 2. Controller 1 ensures the desired process temperature is maintained whereas controller 2 can be used to change the mass flow ratio $\frac{\dot{m}_I}{\dot{m}}$ and seek for favorable operational conditions.

If Controller 2 is not active, the fluid inventory is still actively controlled to offset for leakages and changes in p_1 arising from compressor pressure ratio changes and thermal effects. The pressure p_1 is kept at an operator-defined value $p_{1,\mathrm{set}} = p_{\mathrm{ambient}} + x$, with $x \geq 0$ by injecting dry air from the buffer tank at position 1. The effect can be seen in Fig. 3, test F and G, when controller 2 is inactive. Heat sink mass flow m_I can be manipulated by changing the fan speed in the sink, however, process inlet temperature T_I is the ambient temperature and cannot be changed. Therefore the mass flow has been chosen as parameter for perturbation.

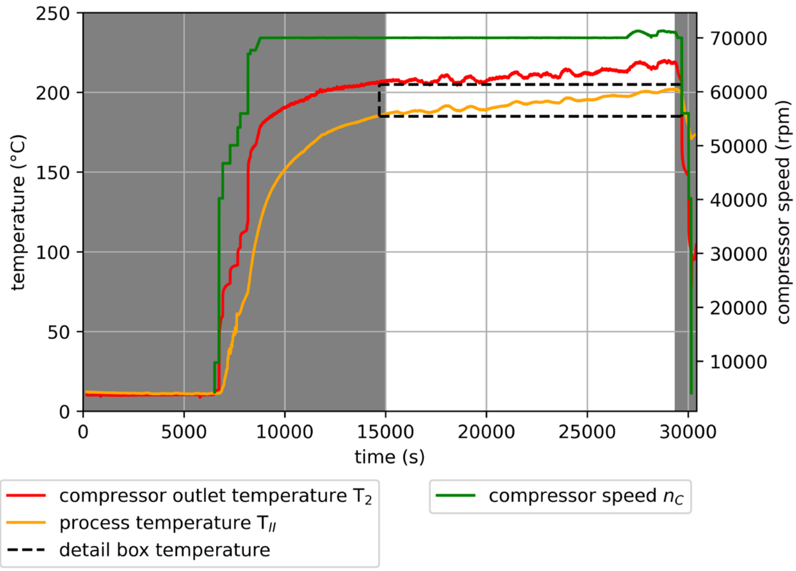

Figure 2: Measured temperature profiles during experiment 1 including start-up and shut-down

3 Results

All data used in this study has been published and is available under CC-BY copyright condition [9]. Experiments 1, 2 and 3 are the test days of 06.02.2025, 24.02.2025 and 25.02.2025 of the publicly available data set respectively. Table 1 gives an overview of the experiments conducted in the scope of this study.

Table 1: Overview experiments

Nr.	Temperature control	COP optimization	Date
1	controller 1 + controller 2	no	2025/02/06
2	controller 1	controller 2	2025/02/24
3	controller 1	manual	2025/02/25

3.1 Experiment 1

In this experiment, the discrete-time, incremental version of controller 1 and controller 2 were evaluated for controlling the process temperature T_{II} of the CoBra heat pump demonstrator. Figure 2 shows the temperature evolution of the compressor outlet temperature T_2 and the process temperature T_{II} for the entire test day including the start-up and shut-down sequence marked in grey. The compressor speed which is the main driver for the heat pump operation and temperature rise is visualized in green. The black dashed area is a sequence with active controllers plotted in more detail in Fig. 3.

In Fig. 3, controller 1 activation is marked by a green area, controller 2 activation by a blue area and temperature setpoints by a black solid line. Controller 1 actively controls the compressor speed (Fig. 3 green line), controller 2 actively controls the compressor inlet pressure p_1 (Fig. 3 blue line). After the start-up sequence is completed, controller 2 is activated with a setpoint temperature of $T_{\mathrm{II,set}} = 188\,°\mathrm{C}$, which is close to the current process temperature T_{II}. The test starts with a perturbation of the process mass flow of roughly 15% induced by varying the fan speed in the heat sink (see Fig. 3 purple line). This test is depicted with 'A' in Fig. 3. Subsequent tests are depicted and referred to in an alphabetical order. Next, the response of controller 2 to four successive set point increases of +2 K each is tested. The control parameters are adjusted after each set point step increase based on the observed system response in order to improve controller performance and reduce overshooting. Table 2 summarizes the applied control parameters for each phase of the experiment. Subsequently, controller 1 is activated to evaluate its response to two set point step increases of +2 K. For the second step increase, the derivative term in the control logic was activated in order to reduce the overshooting. The used control parameters are summarized in Tab. 2.

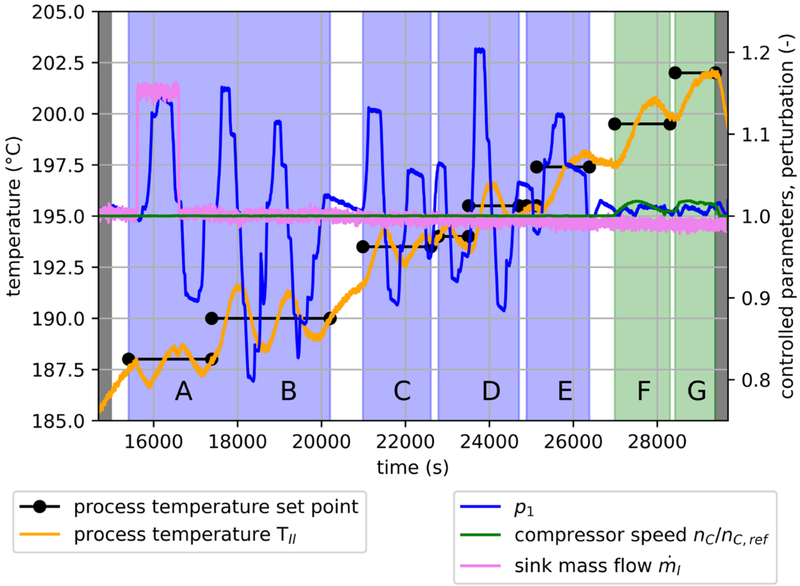

Figure 3: Process temperature experiment 1 with set point temperature and controller activation (green for controller 1, blue for controller 2)

Table 2: Control parameter settings during Experiment 1

	Controller 1				Controller 2			
	K_P	K_d	Δt_1	ΔT_{tol}	K_P	K_d	Δt_2	ΔT_{tol}
A	-	-	-	-	0.02	0	120 s	0.5 K
B	-	-	-	-	0.02	0	120 s	0.5 K
C	-	-	-	-	0.02	2	120 s	0.5 K
D	-	-	-	-	0.02	2	120 s	0.01 K
E	-	-	-	-	0.01	2	120 s	0.01 K
F	100	0	60 s	0.01 K	-	-	-	-
G	100	30000	60 s	0.01 K	-	-	-	-

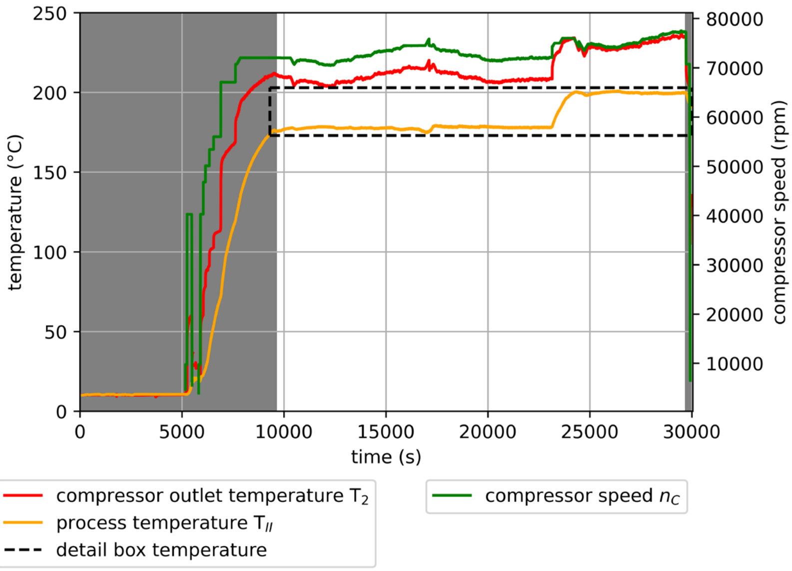

Figure 4: Measured temperature profiles during experiment 2 including start-up and shut-down

3.2 Experiment 2

The results visualized for Experiment 2 follow the same color scheme as described in Sec. 3.1. Figure 4 shows that after start-up, the process temperature T_{II} is kept at 178°C for about three hours and then increased to 200°C. Figure 5 shows the part of the test with active controller. Controller 1 is set to maintain a constant set point temperature of $T_{\mathrm{II,set}} = 178$ °C for about three hours, followed by a second sequence with a set point temperature of $T_{\mathrm{II,set}} = 200$ °C. This experiment utilizes the continuous PID version of controller 1, with a proportional gain of $K_P = 900$, an integral time of $T_i = 360$ s, and a derivative time of $T_d = 0$ s (no derivative part). Controller 2 is active during three different periods. It is used in this experiment to manipulate the fluid inventory in order to find the optimal COP for the given operation with a defined process temperature T_{II}.

To achieve COP optimization, controller 2 adjusts the target compressor inlet pressure (p_1) using a hill-climbing algorithm and then allows the system to settle before measuring the resulting COP. The algorithm continues to change p_1 in the direction that improves the COP, stopping once a peak or system limit is reached and no further improvements are found. Controller 2 does not control the process temperature T_{II}, however it has a perturbing effect on its value which must be offset by controller 1. Figure 5 (purple line) shows the resulting COP during the optimization.

$$\mathrm{COP} = \frac{Q}{P_C - P_T} = \frac{(T_{\mathrm{II}} - T_{\mathrm{I}}) \cdot \dot{m}_I}{(\Delta T_{\mathrm{C}} - \Delta T_{\mathrm{T}}) \cdot \dot{m}} \tag{4}$$

This formula does not account for auxiliary power used for e.g. oil pumps or operating system and uses the compressor and turbine work transferred to the working fluid power for P_C and P_T. It assumes a constant value of specific heat c_{P} for the heat sink and the primary Brayton loop of the heat pump which is a reasonable simplification for air at temperatures of [-50°C, 250°C]. Around t=16500s the compressor inlet pressure reaches p_1=0.7 bara. This low pressure coincides with a sudden rise in compressor oil temperature, a behaviour that the operators have previously observed. Suspected reason is foaming of the lubricant oil and insufficient oil mass flow as a consequence. Hence, the automated fluid inventory controller has to be halted and a higher pressure setting is commanded manually. With the lower pressure limit of $p_{1,\mathrm{min}}$=0.8 bara the automated operation is resumed.

3.3 Experiment 3

The results visualized for Experiment 3 follow the same color scheme as described in Sec. 3.1. Figure 6 shows the evolution of the compressor outlet temperature T_2 and process temperature T_{II}, as well as the compressor speed. The process temperature is kept around $T_{\mathrm{II}} = 200\,^{\circ}\mathrm{C}$ throughout the entire experiment duration except for start-up and shutdown. Figure 7 shows, that the temperature control is managed by controller 1, which is active throughout the experiment with a set point temperature of $T_{\mathrm{II,set}} = 200\,^{\circ}\mathrm{C}$. Controller 1 uses the same controller settings as in Experiment 2 with a proportional gain of $K_P = 900$, an integral time of $T_i = 360$ s, and a derivative time of $T_d = 0$ s. The compressor inlet pressure is modified manually from p_1=1.1 bara to 1.0 bara, 0.9 bara and 0.8 bara. Each pressure setting is maintained for about an hour in order to find the

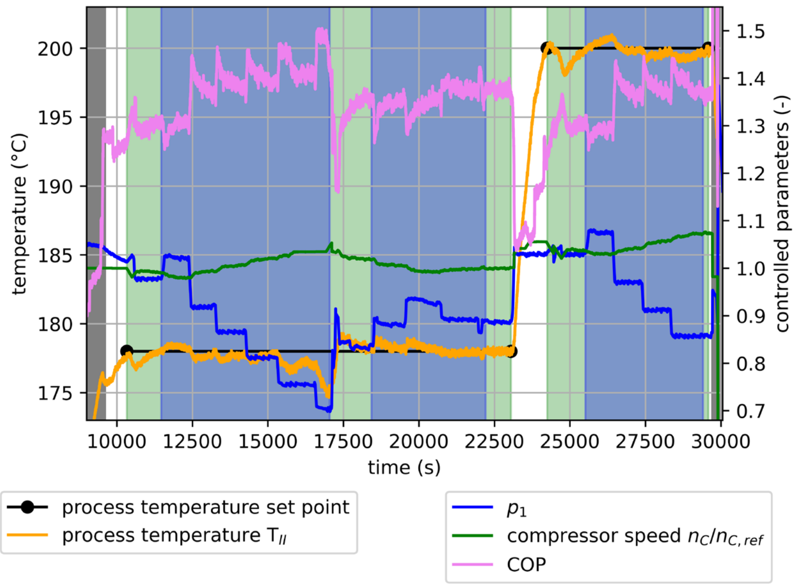

Figure 5: Process temperature experiment 2 with set point temperature and controller activation (green for controller 1, blue for controller 2)

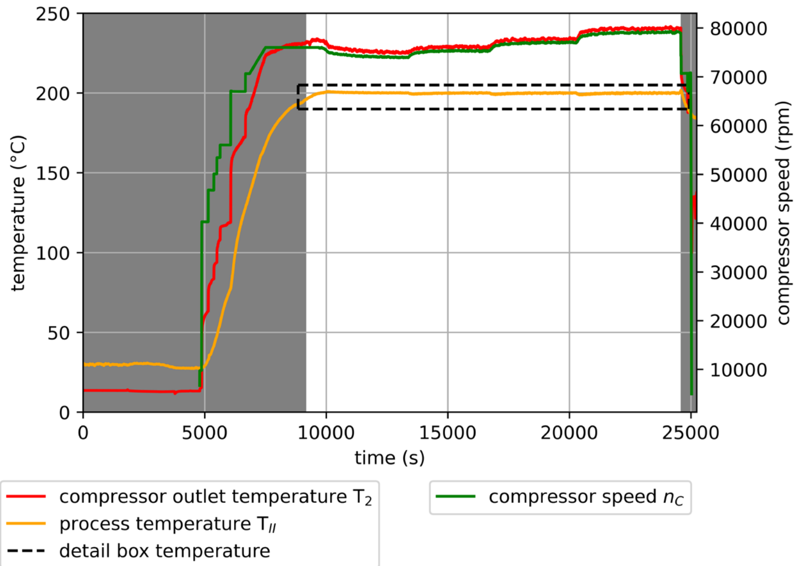

Figure 6: Measured temperature profiles during experiment 3 including start-up and shut-down

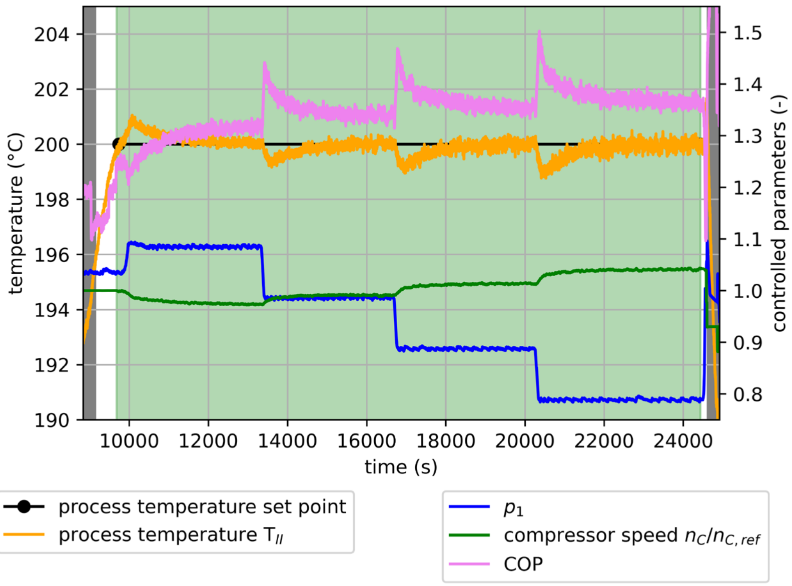

Figure 7: Process temperature experiment 3 with setpoint temperature and controlled parameters

operating conditions with optimal COP. Hold time for constant pressure has been drastically increased with respect to experiment 2 since the operators suspected transients effects to dominate the optimizer routine of experiment 2. To evaluate the controller performance, all three changes in p_1 can be regarded as a perturbation of the dimensionless mass flow ratio $\frac{\dot{m}_I}{\dot{m}}$ by about 10% each.

4 Discussion

The results show that both controllers manage to manipulate process temperature T_{II} such, that it maintains a given set point temperature $T_{\mathrm{II,set}}$ or follows it when set point temperature is increased. After some tuning of controller parameters, both controllers reach the new set point temperature after several minutes without significant overshoot. For perturbations in mass flow ratio of about 10%, the process temperature can be reverted to its desired value in less than 10 minutes with a temperature deviation of less than 2 K. However, it is apparent that e.g. test B and C of controller 2 show unsatisfying controller performance.

Temperatures T_2 and T_{II} both exercise slow transient trends despite constant control inputs even after few hours of operation at similar operating conditions in experiment 1. This is mainly due to the large thermal inertia of the heat exchangers and is supported by other experiments [6] and simulated models [10]. The calculated COP in Experiment 2 also shows variations in absence of any controller action. The authors conclude that the COP has not reached a steady-state value during the COP optimization attempt. Experiment 3 with a waiting time of 1h with constant control inputs still shows a small COP gradient at the end of every sequence with constant control inputs. Therefore no reliable conclusion on the COP optimal operation can be made with this data set. A repetition of this test is planned.

Experiments 2 and 3 show that constant process temperature can be maintained after a reduction in FI with a controller-induced increase in compressor speed. Reduction of fluid inventory and increase in compressor speed can thus compensate each others effect on the process temperature.

4.1 Set point variation

In Test B a set point change of +2 K of controller 2 leads to an overshoot of +1.7 K and a second overshoot of +1.3 K. Thus, significant oscillation around the set point temperature and little damping is present. The oscillation period is 20 minutes. This controller performance is poor when compared to the subsequent tests C, D and E. Parameters are subsequently tuned (see Tab. 2 to reduce overshoot and make T_{II} converge to its set point quickly. In Test E which yields the best result, the new temperature set point is reached within 12 minutes and the overshoot is less than 0.5 K. This shows that a fluid inventory controller can be used in order to achieve small changes of process air temperature. A reduction of the proportional gain K_P substantially reduced the overshoot. Controller 1 also achieves the task of a set point increase of +2 K. The controller settings in test F lead to an overshoot of 1 K. Test G using a derivative gain K_d yields the best results, reaching the set point temperature within 10 minutes with no overshoot and very precise temperature control.

The varying performance in experiment 1 shows clearly that appropriate controller parameters are important for a good controller performance. A more systematic investigation of controller parameters is necessary to derive more general conclusions on Brayton heat pump control.

4.2 Response to perturbation

In Test A, controller 2 is able to maintain the set point temperature with a maximum deviation of about 1.1 K after a perturbation of mass flow ratio $\frac{\dot{m}_\mathrm{I}}{\dot{m}}$ of 15%. This holds both for a positive and negative change. From the trend in pressure p_1 and mass flow m_I (see Fig. 3) which are both linearly linked to the numerator and denominator of the mass flow ratio $\frac{\dot{m}_\mathrm{I}}{\dot{m}}$ one can derive that controller 2 tends to maintain a constant mass flow ratio. After the sink mass flow increase $\dot{m}_\mathrm{I}$, the controller directly increases p_1 to a similar level, which leads to a Brayton loop mass flow increase $\dot{m}$of the same magnitude. Controlling the fluid inventory of the heat pump seems a promising approach for responding to a change in process mass flow with constant temperature requirements. The ability of supplying different process mass flows at a constant supply temperature as well as a constant COP has also been shown by Oehler et al. [6]. Experiments 2 and 3 show the response of controller 1 to perturbations of the mass flow rartio $\frac{\dot{m}_\mathrm{I}}{\dot{m}}$. The mass flow in the Brayton loop $\dot{m}$ is linearly linked to the compressor inlet pressure p_1 plotted in Fig. 5 and Fig 7. The temperature can be kept within $\pm 1.5\,K$ for the whole test period of both experiments even when mass flow ratio changes of about 10% occur due to fluid inventory changes. The only exception happens in experiment 2 around t=16500 s. The process temperature deviation is due to a limitation in the autonomy of the controller. Around t=16000 s the compressor speed controller is restricted by its upper limit of $n_{C,max}$ = 75 krpm. As soon as this limit is elevated around t=17000 s the temperature stabilizes again at the set point $T_\mathrm{II,set}$ = 178°C. Allowing more autonomy for the controller could therefore yield faster reaction times and better overall controller performance.

5 Conclusion

The experimental results suggest that the applied control strategies "compressor speed control" and "fluid inventory control" can both keep the process temperature constant during minor perturbations of the process mass flow or heat pump mass flow of a Brayton-cycle HTHP. Small changes of the desired process temperature can also be realized with both controllers. The results of this study suggest that controlling the compressor speed yields better controller results in terms of reaction speed and accuracy. Both controllers were able to compensate for changes in the mass flow ratio $\frac{\dot{m}_\mathrm{I}}{\dot{m}}$ of over 10% without impacting process temperature by more than 2 K. The current controller setup is constraint by minimum and maximum values as well as minimum and maximum gradients for the controlled variables. However, controller performance could be increased by removing these restrictions. A constant process temperature can be maintained despite a reduction in FI with an increase in compressor speed.

6 Outlook

The limits of the applied controllers will be tested for sudden process mass flow changes as big as 50%. Further testing is also planned with more substantial temperature set point increases of 10 K and more. It should be further investigated whether FIC yields advantages over the more traditional compressor speed controller. Automization of the start-up and shut-down routine, as well as developing a robust controller that achieves safe and stable operation at optimum COP are the future research goals of the CoBra group. This will require a more systematic tuning of the controller parameters.

References

[1] IRENA, *World energy transitions outlook 2023 : 1.5°C pathway.* [Abu Dhabi]: International Renewable Energy Agency IRENA, 2023.

[2] EDGAR, "Emissions database for global atmospheric research community ghg database," 2024. `https://edgar.jrc.ec.europa.eu/report_2024`.

[3] Heat Pump Centre, "Iea hpt annex 58: High-temperature heat pumps," 2023.

[4] R. Wang, X. Wang, G. Shu, H. Tian, J. Cai, X. Bian, X. Li, Z. Qin, and L. Shi, "Comparison of different load-following control strategies of a sco2 brayton cycle under full load range," *Energy*, vol. 246, p. 123378, 2022.

[5] M. Pettinari, G. F. Frate, L. Ferrari, F. C. Yücel, A. P. Tran, P. Stathopoulos, and K. G. Kyprianidis, "Thermal load control in high-temperature heat pumps: a comparative study," *Journal of Engineering for Gas Turbines and Power*, pp. 1–40, 2024.

[6] J. Oehler, F. C. Yücel, and P. Stathopoulos, "Experimental performance analysis of a 50 kw brayton turbomachine heat pump demonstrator," in *Volume 4: Controls, Diagnostics & Instrumentation; Cycle Innovations; Education; Electric Power*, American Society of Mechanical Engineers, 2025.

[7] A. P. Tran and F. C. Yücel, "Safe and efficient control of a brayton cycle heat pump using reinforcement learning," in *Proceedings of the 16th International Modelica&FMI Conference, September 8 – 10, 2025, Lucerne University of Applied Sciences and Arts (HSLU)*, Linköping Electronic Conference Proceedings, Linköping University Electronic Press, 2025.

[8] F. C. Yücel, J. Oehler, M. Kriese, E. Jende, N. Setzepfand, and P. Stathopoulos, "Design, commissioning and closed-loop operation of a high-temperature brayton heat pump–cobra," *Applied Thermal Engineering*, p. 127947, 2025.

[9] J. Oehler, J. Naumann, F. C. Yücel, P. Tran, N. Uddin, N. Setzepfand, M. Tannert, J. Herbrich, P. Stathopoulos, and Department of High-Temperature Heat Pumps, "Cobra high temperature heat pump demonstrator - experimental dataset 2024-2025," 2025.

[10] J. Oehler, A. P. Tran, and P. Stathopoulos, "Simulation of a safe start-up maneuver for a brayton heat pump," in *Volume 4: Cycle Innovations; Cycle Innovations: Energy Storage*, American Society of Mechanical Engineers, 2022.